Supporting Information

An Oxygen-scavenging System without Impact on DNA Mechanical Properties in Single-Molecule Fluorescence Experiments

Shang Gao, [a,b] Jialun Liang, [a,b] Chuang Tan* [a,b] and Jie Ma *[a,b]

[a] School of Physics, Sun Yat-sen University, Guangzhou 510275, People's Republic of China.

[b] State Key Laboratory of Optoelectronic Materials and Technologies, Sun Yat-sen University, Guangzhou 510006, China.

* Corresponding author. Email: majie6@mail.sysu.edu.cn;

tanch26@mail.sysu.edu.cn.

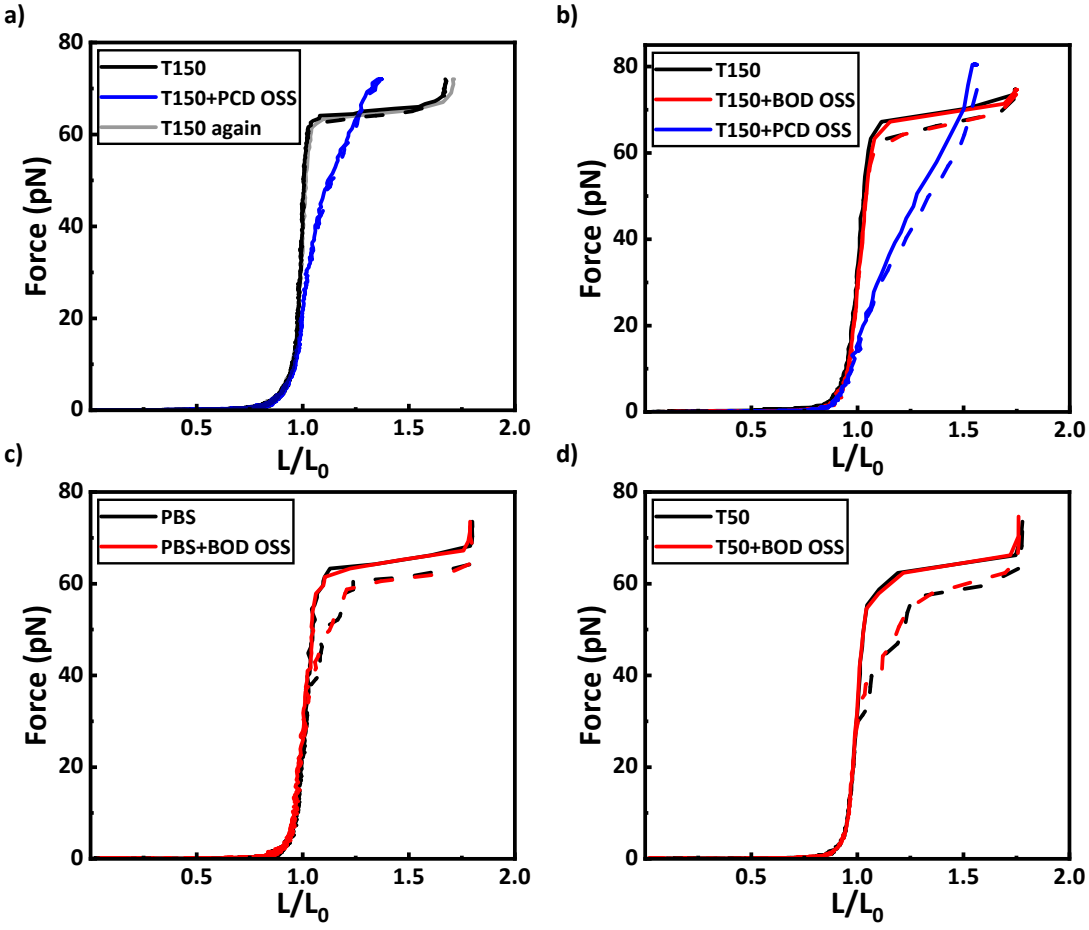

Figure S1. Effects of the PCD and BOD oxygen-scavenging systems (OSSs) in different buffers on the force-extension curve (FEC) of a single DNA molecule. (a) Representative FECs of the same DNA molecule measured successively in T150, T150 with PCD OSS, and T150 again. The horizontal axis represents the ratio of DNA length to its contour length, while the vertical axis indicates the force applied to the DNA by magnetic tweezers. (b) Representative FECs of the same DNA molecule measured successively in T150, T150 with BOD OSS, and T150 with PCD OSS. (c, d) FECs of DNA measured in (c) PBS or (d) T50 buffer with (red) or without (black) BOD OSS. Notice here that the solid lines represent the stretching curves and the dashed lines represent the relaxing curves.

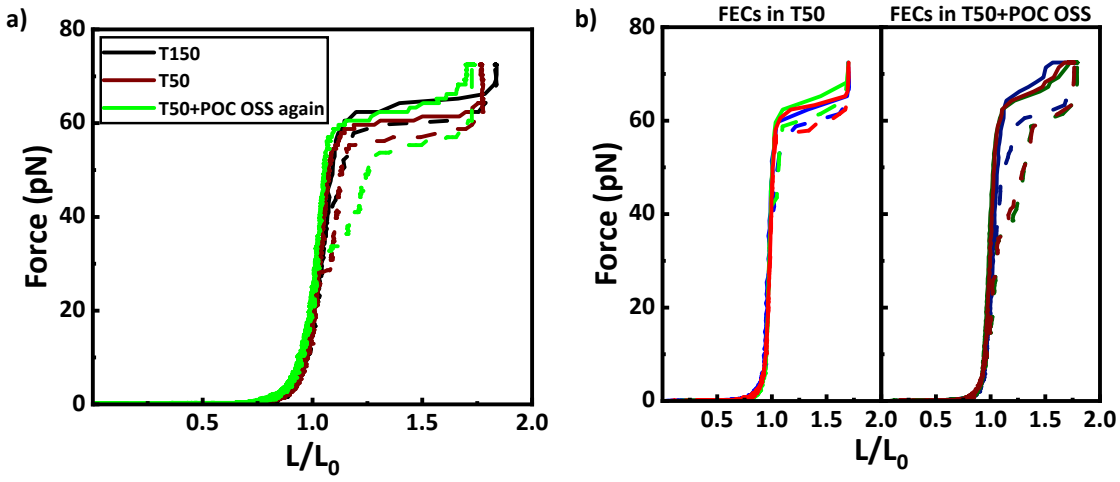

Figure S2. The effect of POC OSS on the DNA FECs in different buffers. (a) Representative FECs of the same DNA molecule measured successively in T150, T50, and T50 with PCD OSS. (b) Representative FECs of different DNA molecules in T50 buffer without (left panel) and with (right panel) POC OSS. Different colors represent different DNA molecules. The solid lines represent the stretching curves while the dashed lines correspond to the relaxing curves.

Table S1. The overstretching transition force ($F_{overstretching}$) and hysteresis energy for DNA measured in different buffers (T150, T50, and T50 with POC OSS). The values of $F_{overstretching}$ are obtained by averaging forces in the overstretching transition region, and the values of hysteresis energy are derived by subtracting the integral of the relaxing curve from the stretching curve over the range of 10–80 pN. All values are presented as mean ± SE measured from 30 tethers.

	T150	T50	T50+POC OSS
$F_{overstretching}$ (pN)	66.5±0.9	62.9±0.5	66.6±0.3
Hysteresis energy (pN·nm)	5990.7±173.7	6298.5±113.6	15266.5±1091.3

Table S2. Parameters obtained from fitting DNA FECs with a modified Marko-Siggia Worm-Like-Chain (WLC) model[1] (0-30 pN). All values are presented as mean ± SE.

	L_0 (nm)	L_p (nm)	K (pN)	N
T50	1713.9±13.1	34.1±4.3	679.3±40.2	32
T50BOD	1700.1±9.5	37±1.9	613.8±41.3	94
T50PCD	1725.6±10.9	42.4±4.2	507.2±30.2	42
T50POC	1727.6±14.8	34.6±4.6	793.2±42.8	27
PBS	1723.4±6.3	37.6±2.6	809.5±59.1	64
PBSBOD	1707.8±8.9	39.8±1.5	811.5±25.3	86
PBSPCD	1722.5±4.8	45.8±2.4	578±15.1	28
PBSPOC	1706.6±6.8	39.7±9.1	853.3±58.1	33

*N represents the number of traces used for statistical analysis.

Investigation on the mechanisms for PCD and POC oxygen-scavenging systems to affect DNA mechanical properties

We conducted further studies to investigate the mechanisms for PCD OSS and POC OSS to modify the mechanical properties of DNA. Regarding to PCD OSS, we first examined its individual components, including PCA, Trolox (a quencher for dye triplets), and the PCD enzyme. Each component was added separately to the T150 buffer, and none of these components alone had any significant impact on the FEC, as shown in Figure S3a. This result ruled out the possibility that the observed perturbation arises from individual reactants in the PCD OSS. It also excluded the likelihood that the altered FEC is due to unknown impurities in the purified PCD enzyme, as previously reported[2]. Next, we tested combinations of reactants (PCA+Trolox, PCD+Trolox and PCA+PCD), and found that only PCA+PCD pair modified the FEC, as shown in Figure S3b, ruling out Trolox as a contributor to the perturbation of DNA mechanical properties. These results suggest that a product of the PCA-catalyzed reaction by PCD impacts the mechanical properties of DNA. We hypothesized that hydrogen ion (H^+) from the reaction products might influence the measured FECs. However, varying the pH of T150 buffer from 8.0 to 6.0 without OSS led to only minor changes in the DNA FECs (see Figure S3c), with a slight (<1pN) shift in the overstretching transition force[3], which was distinct from the effects observed with PCD OSS (see Figure 2a). As a result, the other product from PCD OSS reaction, 3-carboxy-cis, cis-muconic acid, seemed to be more likely to account for the modified FECs of DNA.

Given that 3-carboxy-cis, cis-muconic acid is negatively charged in its deprotonated form (see Figure 1), it is unlikely to bind DNA via electrostatic interactions. Interestingly, the FECs observed with PCD OSS are similar to those reported for DNA in the presence of certain intercalative ligands[4, 5]. To examine whether 3-carboxy-cis, cis-muconic acid might bind to DNA through intercalation, we conducted DNA twisting experiments by winding the same DNA in T150 buffer without OSS and T150 buffer with different OSSs under a constant force of ~ 0.27 pN. As shown in Figure S4, the DNA twisting curves were nearly unchanged upon introducing PCD OSS, ruling out the possibility that 3-carboxy-cis, cis-muconic acid acts as a typical DNA intercalator, which would supercoil the torsionally-constraint DNA under zero force[5, 6]. We then explored whether 3-carboxy-cis, cis-muconic acid might interact with DNA through the minor or major groove, potentially forming hydrogen bonds with exposed bases through its oxygen atoms. However, in its negatively charged, deprotonated form (Figure 1), 3-carboxy-cis, cis-muconic acid encounters significant challenges in directly binding to DNA. Thus, we propose that the catalytic reaction in PCD OSS might proceed in a pathway as shown in Figure S5. Based on this, we hypothesized that the molecule's binding affinity to DNA might increase under acidic conditions when it is protonated. To test this hypothesis, we measured the force-extension curves with and without PCD OSS under various pH buffer conditions. T50 buffer was used instead of T150 buffer because, at lower salt concentrations, the charge-screening effect is weaker, making the deprotonated form of 3-carboxy-cis, cis-muconic acid less likely to bind DNA and rendering the binding process more sensitive to pH

changes. The results are presented in Figure S6 and S7. As illustrated in Figure S6, lowering the pH from 7.0 to 6.0 in T50 buffer without PCD OSS had minimal impact on DNA FECs, consistent with previous observations in T150 buffer (Figure S3c). However, as illustrated in Figure S7, FECs in the presence of PCD OSS exhibited more significant changes at lower pH, suggesting enhanced binding affinity for 3-carboxy-cis, cis-muconic acid under acidic conditions. Furthermore, as depicted in Figures 2a, S3b, and S7, the effect of PCD OSS on the DNA FECs was force-dependent, with more pronounced alterations under higher tension. This may result from increased exposure of DNA bases at higher forces, facilitating their interactions with 3-carboxy-cis, cis-muconic acid.

Regarding POC OSS, the addition of its substrate (glucose) to the solution exhibited no influence on the measured FEC in both T150 and T50 buffers (see Figure S8a and S8b). Considering that reducing the salt concentration from 150 mM to 50 mM (i.e., changing buffer from T150 to T50) induced significant hysteresis in the DNA stretching and relaxing curves upon introducing POC OSS, we hypothesize that some reagent within POC OSS potentially interacts with single-stranded DNA (ssDNA). Under low salt conditions, the diminished efficiency of charge screening makes DNA more prone to force-induced unpeeling, encouraging the reagent's binding to ssDNA. Subsequently, the unpeeled DNA segments encounter difficulties in reannealing, contributing to the notable hysteresis observed in the DNA stretching and relaxing curves.

Finally, though our experiments provide some useful insights and clues for elucidating the underlying mechanisms for PCD and POC OSSs to influence DNA mechanical

responses, more direct evidences from structural analysis using NMR or X-ray crystallography are essential in order to draw a clear conclusion in the future.

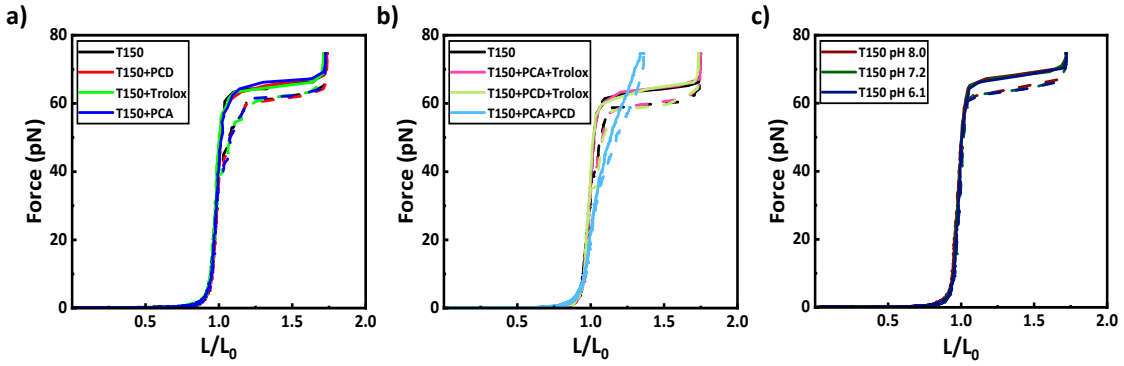

Figure S3. DNA stretching experiments in various solutions to investigate the mechanism by which the PCD OSS influences the mechanical properties of DNA. (a) FECs of the same DNA molecule in T150 buffer without PCD OSS (black) or with individual PCD OSS components: protocatechuate 3,4-dioxygenase (PCD, red), Trolox (green), and 3,4-dihydroxybenzoic acid (PCA, blue). (b) Similar to (a), but with pairs of components added: PCA+Trolox (light red), PCD+Trolox (light green), and PCA+PCD (light blue). (c) FECs of the same DNA molecule in T150 buffer (without OSS) at different pH values: pH=8.0 (dark red), pH=7.2 (dark green), pH=6.1 (dark blue).

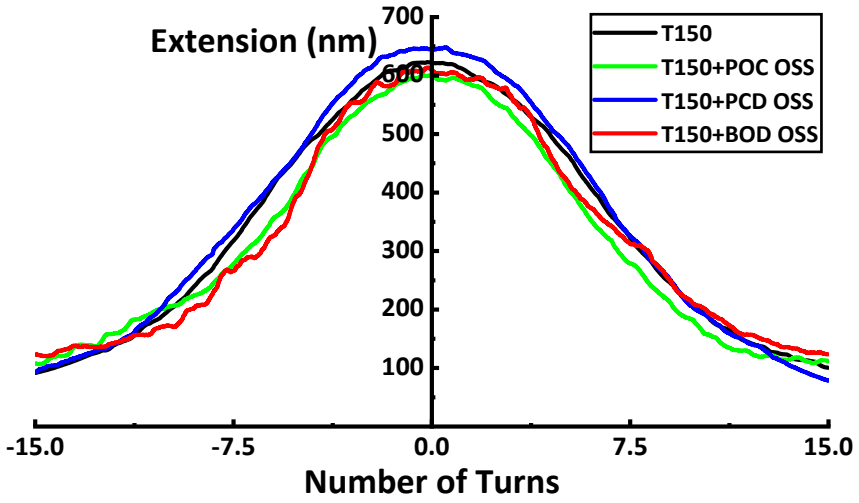

Figure S4. Typical winding curves of the same DNA molecule in T150 buffer (black), and T150 buffer with POC OSS (green), PCD OSS (blue), or BOD OSS (red).

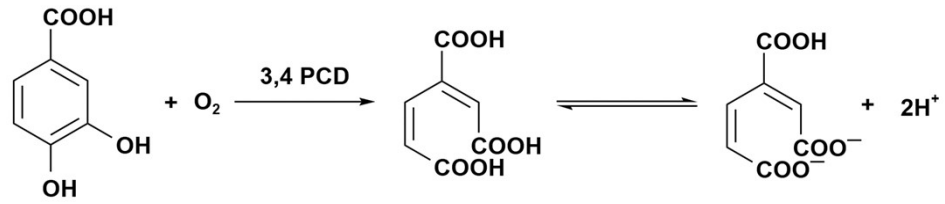

Figure S5. Proposed reaction pathway for PCD OSS. The reaction product, i.e., 3-carboxy-cis, cis-muconic acid, may exist in either protonated or deprotonated form depending on the pH of the solution.

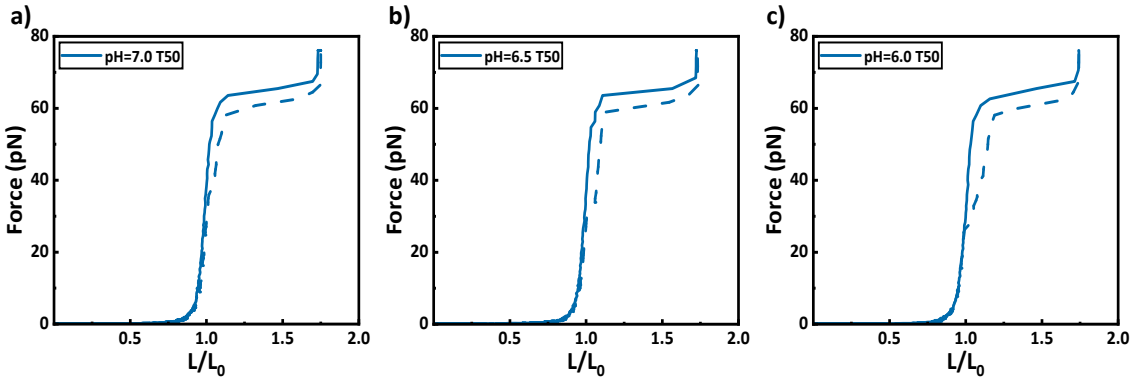

Figure S6. Force-extension curves of the same DNA molecule in T50 buffer (without OSS) at different pH values: (a) pH=7.0, (b) pH=6.5, (c) pH=6.0. Minimal changes in the DNA FECs were observed as the pH of the buffer decreased from 7.0 to 6.0.

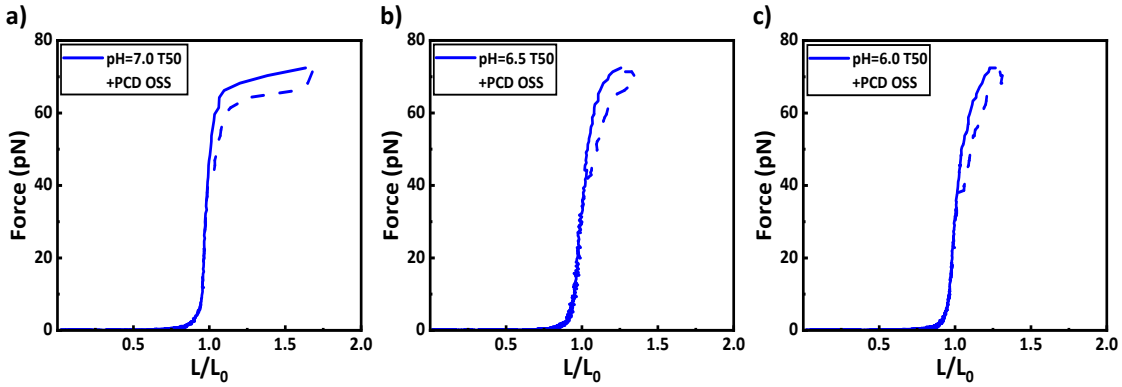

Figure S7. FECs of the same DNA molecule in T50 buffer with PCD OSS at different pH values: (a) pH=7.0, (b) pH=6.5, (c) pH=6.0. FECs showed more pronounced modifications as the pH of the buffer was lowered from 7.0 to 6.0.

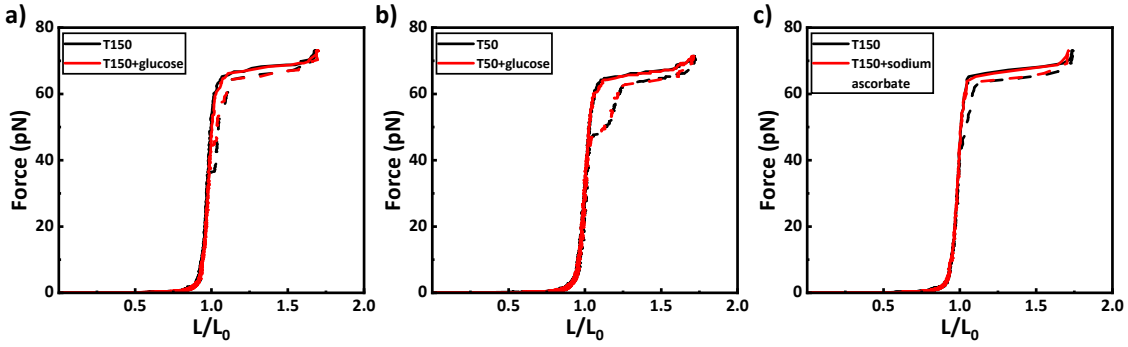

Figure S8. Effects of substrates in POC OSS and BOD OSS on DNA FECs. (a) FECs of the same DNA molecule before (black) and after (red) introducing the POC OSS substrate (glucose) into T150 buffer. (b) Similar to (a), but with glucose added under low salt (T50 buffer) conditions. (c) FECs of the same DNA molecule before (black) and after (red) introducing BOD OSS substrate (sodium ascorbate) into T150 buffer. Here, the solid lines represent the stretching curves while the dashed lines correspond to the relaxing curves.

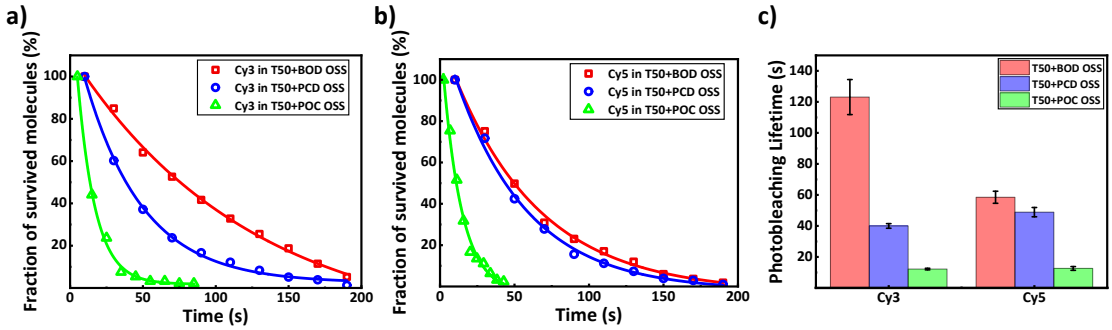

Figure S9. Single-molecule fluorescence experiments to assess OSS effects on the photobleaching lifetimes of dyes in T50 buffer. (a, b) Survival fraction curves of (a) Cy3 and (b) Cy5 obtained with BOD OSS (red), PCD OSS (blue) and POC OSS (green). Each curve was calculated from over 90 single-molecule fluorescence trajectories, with survival fractions representing the percentage of fluorescent molecules not photobleached at

various time slots after excitation. The characteristic photobleaching lifetime was determined via a single exponential fit (solid line) to the survival fraction decay curve. (c) Photobleaching lifetimes of Cy3 and Cy5 fluorophores in T50 buffer with different OSSs, as obtained from (a) and (b). The error bars represent SE from fitting.

Table S3. Photobleaching lifetimes of Cy3 and Cy5 fluorophores in T50 buffer with different OSSs. The values are presented as mean ± SE, with the number of traces used for statistical analysis shown in parentheses.

	BOD OSS	PCD OSS	POC OSS
Cy3	123.1±11.3 s (192)	40±1.5 s (156)	12.2±0.5 s (93)
Cy5	58.5±3.9 s (217)	48.9±3.0 s (205)	12.6±1.2 s (126)

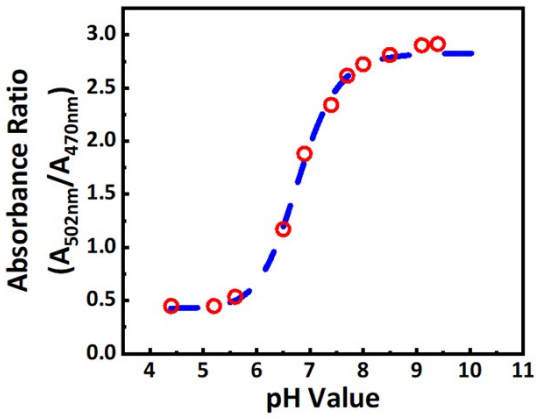

Figure S10. Calibrated relationship between absorbance ratio (A_{502nm}/A_{470nm}) and pH value, using solutions with known pH values (measured with an acidometer) and a Spexyte™ Micro pH Probe. Red circles represent experimental data, and the blue dashed line indicates the fitting curve.

The expression for the fitting curve is given by：

$$Absorbance\ Ratio = 0.426 + \frac{2.402}{1 + \left(\frac{pH}{6.781}\right)^{-17.926}}$$

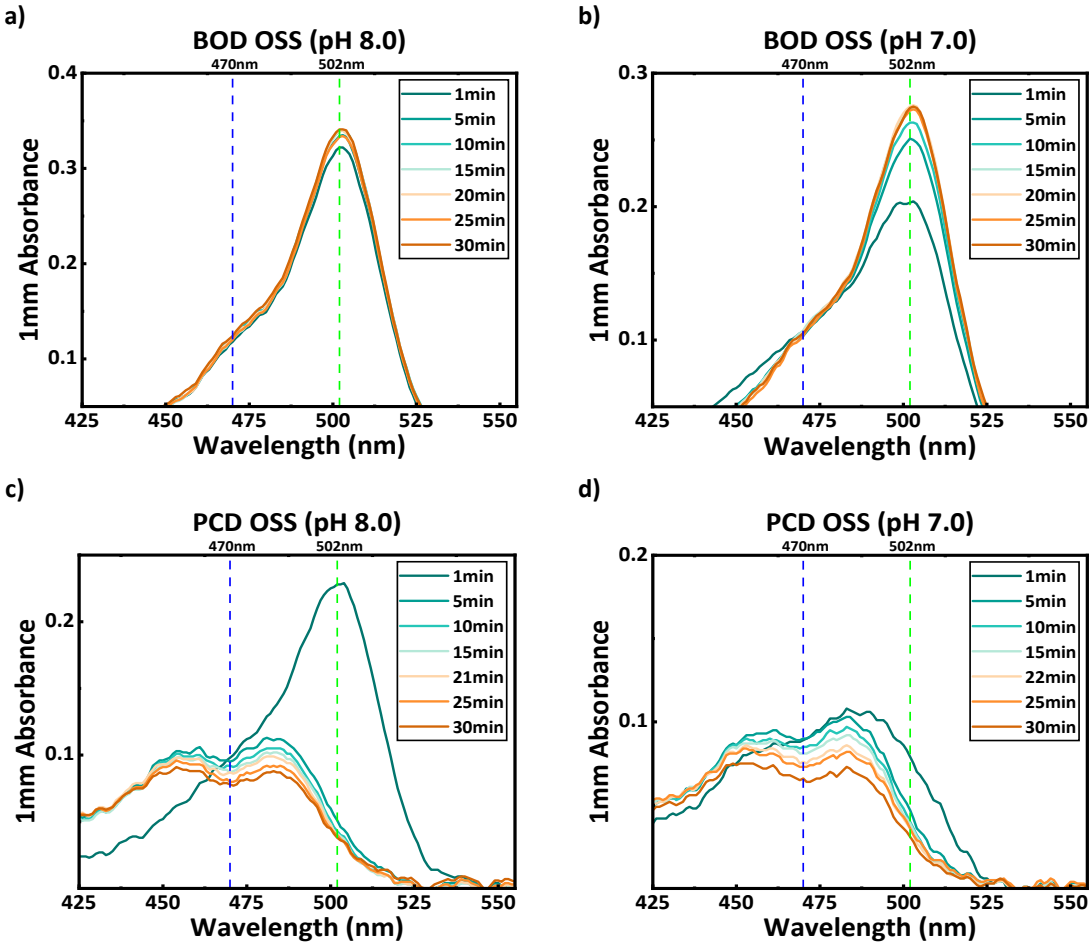

Figure S11. Changes in the absorption spectrum of the Spexyte™ Micro pH probe over a 30-minute period following the addition of BOD OSS or PCD OSS to T150, starting from different initial pH values:(a) BOD OSS added to T150 buffer (initial pH = 8.0), (b) BOD OSS added to T150 buffer (initial pH = 7.0), (c) PCD OSS added to T150 buffer (initial pH = 8.0), (d) PCD OSS added to T150 buffer (initial pH = 7.0).

References：

1. C. Bouchiat, M. D. Wang, J.-F. Allemand, T. Strick, S. M. Block and V. Croquette, *Biophysical Journal,* 1999, **76**, 409-413.
2. G. Senavirathne, J. Liu, M. A. Lopez, J. Hanne, J. Martin-Lopez, J.-B. Lee, K. E. Yoder and R. Fishel, *Nature Methods*, 2015, **12**, 901-902.
3. M. C. Williams, I. Rouzina and V. A. Bloomfield, *Accounts of chemical research*, 2002, **35**, 159-166.
4. I. D. Vladescu, M. J. McCauley, M. E. Nuñez, I. Rouzina and M. C. Williams, *Nature methods*, 2007, **4**, 517-522.
5. A. A. Almaqwashi, T. Paramanathan, I. Rouzina and M. C. Williams, *Nucleic acids research*, 2016, **44**, 3971-3988.
6. J. Lipfert, S. Klijnhout and N. H. Dekker, *Nucleic acids research*, 2010, **38**, 7122-7132.